Advances in Science and Technology Research Journal

Advances in Science and Technology Research Journal 2023, 17(6), 88–97
https://doi.org/10.12913/22998624/174180
ISSN 2299-8624, License CC-BY 4.0

Received: 2023.09.26
Accepted: 2023.10.15
Published: 2023.11.21

Study of Crystalline and Thermal Properties of Nanocomposites Based on Polyamide-6 and Modified Montmorillonite

Volodymyr Krasinskyi[1,2*], Ludmila Dulebova[3], Ivan Gajdos[3], Oksana Krasinska[1], Tomasz Jachowicz[4]

[1] Lukasiewicz Research Network – Institute for Engineering of Polymer Materials and Dyes, M. Skłodowska-Curie 55 St., 87-100 Torun, Poland

[2] Lviv Polytechnic National University, Department of Chemical Technology of Plastics Processing, Bandera 12 St., 79013 Lviv, Ukraine

[3] Technical University of Košice, Faculty of Mechanical Engineering, Department Technologies, Materials and Computer Aided Production, Masiarska 74 St., 04001 Košice, Slovakia

[4] Lublin University of Technology, Faculty of Mechanical Engineering, Department of Polymer Processing, Nadbystrzycka 36 St., 20-618 Lublin, Poland

* Corresponding author's e-mail: vkrasinsky82@gmail.com

ABSTRACT

The main operational characteristics of polyamide-6-montmorillonite (PA6/MMT) nanocomposites, which determine their fields of application, mainly depend on the crystal structure and crystallinity of the polymer. Therefore, the study of the crystalline behavior of PA6 in such nanocomposites is of considerable scientific and practical importance. In this work, the structure, crystalline, and thermal properties of nanocomposites based on PA6 and modified MMT prepared in a formic acid solution were investigated using the methods of differential scanning calorimetry (DSC) and X-ray Diffraction (XRD). It was established that during the manufacture of PA6/MMT nanocomposites in a solution, the dominant crystal structures are the thermodynamically stable α structures of PA6. The crystallinity degree of PA6 in nanocomposites is about 1.5 times higher than that of the original PA6. It is shown that after additional thermomechanical treatment of nanocomposites on a capillary viscometer at 230 °C and a load of 5 kg, the uniformity of the distribution of exfoliated MMT in the polymer matrix increases, as a result of which the crystalline structure of PA6 changes and its glass transition and melting temperatures increase. These changes in the PA6 structure also have a significant impact on the melt flow index and the softening temperature of nanocomposites.

Keywords: nanocomposites, polyamides, thermal properties, crystal structures, processing.

INTRODUCTION

Nanocomposite materials basis on clay nanolayers (typically MMT) and polymeric matrices demonstrate excellent performance characteristics suitable for sophisticated industrial applications [1–6]. In particular, Cheira et al. obtained highly effective adsorbents based on PA6/MMT nanocomposites (by the melt mixing method) for U(VI) adsorption from aqueous solutions [7]. The polymer-clay nanocomposites may be obtained mainly by three methods: intercalation of a suitable monomer followed by polymerization [8, 9]. polymer intercalation from solution, [10] and direct polymer melt intercalation [11]. Nanocomposite materials have attracted great interest because nanoclays can reinforce almost all types of polymer matrices with similar properties to traditional composites but with less weight and better processability [12, 13].

The thermal and mechanical characteristics of polyamide and polymer–clay nanocomposite

are greatly influenced by crystal structure [14–19]. For example, during the crystallization of PA6, three forms of crystals α, β, and γ can be formed. The stable monoclinic α structure organizes in planar zigzag chains, whereas the metastable, pseudo-hexagonal γ structure is organized in a twisted chain [20–22]. The mesomorphic β-structure is little known and is considered an intermediate state between the first two [23–26].

The fields of industrial applications of PA6/MMT nanocomposites are determined by their physical and mechanical properties, which, in turn, depend on the structure and crystallinity of the polymer matrix. Yebra-Rodríguez et al. [1] used DSC analysis and thermo-X-ray diffraction routines for 2D mapping to study the effect of temperature on the crystal structure of PA6/MMT nanocomposites. Organically modified MMT increases the thermal stability of PA6 and promotes the genesis of the thermodynamically unstable γ crystalline phase.

Sun et al. [27] established that MMT particles are crucial during the heterogeneous nucleation of PA6, as a result of which the crystallization temperature of nanocomposites obtained by mixing in a melt using Hakke rheometer increases. The α crystals are predominant crystal structures in pure PA6 and nanocomposite, but the γ crystals appear during the melting process.

Lin et al. [28] reported that multiple melt mixing positively affects the dispersion of silicate layers and the mechanical properties of PA6/MMT nanocomposites. At the same time, as a result of the partial destruction of PA6, the impact strength and relative elongation at break of nanocomposites decrease. As the number of melt mixing cycles increases, the melting point of PA6 decreases, and its crystallization temperature increases.

Monticelli et al. [29] established the influence of commercial grades of organo-MMT obtained by melt mixing and in situ polymerization on the properties and structure of PA6. The final nanocomposite characteristics, such as MMT particle distribution, molecular weight, and the crystallinity degree of PA6, depended on the type of clay and the method of obtaining composites. Moreover, one of the main factors affecting the characteristics of the nanocomposite is the stability of the organic clay modifier at the processing temperature.

Thus, to obtain polymer nanocomposites with the required characteristics, it is necessary to have a complete comprehension of the interfacial phenomena between the nanofiller particles and the polymer matrix. Namely, crystallization conditions are one of the crucial factors affecting the crystal structure, thermal behavior, and mechanical properties of polymer (nano)composites.

This work aimed to investigate the structure, crystallization behavior, and thermal properties of PA6/MMT nanocomposites obtained in a solution and to analyze the effect of additional thermomechanical processing of composites on these characteristics. The XRD and DSC methods were used for research. MMT modified with polyvinylpyrrolidone (PVP) was used to obtain nanocomposites based on PA6 [30].

MATERIALS AND METHODS

Materials

PA6-210/310 brand (Grodno-Azot, Belarus) with melting temperature 215 °C, melt flow index 19 g/10 min (230 °C/2.16 kg). MMT [$Al_2Si_4O_{10}(OH)_2 \cdot nH_2O$] (69911, Sigma-Aldrich), untreated, with polydisperse particles 150–300 nm in size, in the form of agglomerates 3-20 μm, specific surface area of 250–270 m^2/g, bulk density of 300–370 kg/m^3. PVP 10, purchased from Duchefa Biochemie (P1368), Netherlands, with a molecular weight average of 10000 g/mol, a density of 1.200 kg/m^3, and a bulk density from 400 to 600 kg/m^3. Benzene (99.6%, Sigma-Aldrich), acetone (99.5%, Sigma-Aldrich), and formic acid (85%, Sigma-Aldrich) were applied.

Sample preparation

To improve the compatibility of MMT with thermoplastic polymers, it was pre-intercalated with PVP with the MMT:PVP ratio equal to 1:5 (MMT-PVP) in an aqueous solution in an ultrasonic field [30]. The PA6/MMT-PVP-based nanocomposite was obtained as follows [2]. Using an electromagnetic stirrer, 15% solutions of PA6 in formic acid (85%) were prepared. Mixing was carried out without heating until the complete dissolution of PA6. Then, MMT-PVP was added to the solutions in amounts of 5, 10, and 20 wt% (relative to the mass of dry PA6). Stirring was continued until a stable colloidal solution was formed. The resulting nanopolymer complex was precipitated with an acetone-benzene mixture

(1:1 by volume), filtered, and washed with acetone. Next, the nanocomposites were dried in a vacuum at 100 °C for 7 hours. The finished products were obtained as a white finely dispersed powder. As a comparison sample, pure PA6 was obtained similarly.

To study the effect of additional thermomechanical processing on the characteristics of the obtained nanocomposites, they were subjected to shear deformation on the capillary viscometer IIRT-AM (ASMA-Pribor, Ukraine) at 230±5 °C and a load of 5 kg.

Test methods

The PA6/MMT nanocomposites were identified via XRD using PANalytical Empyrean diffractometer (Malvern Panalytical, UK) with CuKα radiation (1.54056 Å), tube voltage of 45 kV, tube current of 40 mA. Measurements were made within angles 5–60° with a step size of 0.017° and a counting rate of 15 s/step.

Thermal studies were performed using a differential scanning calorimeter SDT Q600 (TA Instruments, USA). The sample mass loss (TGA) and the thermal processes (DSC) occurring in the sample during heating from 20 to 300 °C (heating rate of 5 °C/min) were recorded simultaneously. The measurements were carried out in an argon atmosphere (the sample mass was 8-10 mg). Universal V4.5A TA Instruments program was used to analyze the obtained data and calculate the crystallinity degree of PA6, accepting that the thermodynamic fusion enthalpy of 100 % crystalline PA6 amount of 230 J/g [31, 32].

The melt flow index of the nanocomposites was measured (at 230 °C, a load of 2.16 kg) on a capillary viscometer IIRT-AM (ASMA-Pribor, Ukraine). The Vicat softening temperature was measured using a Hepler consistometer (heating rate of 1 °C/min, load of 50 N).

RESULTS AND DISCUSSION

The X-ray diffractograms for the nanocomposites PA6/MMT-PVP (with amounts of MMT-PVP 5, 10, and 20 wt%) and original PA6 obtained in a formic acid solution are presented in Figure 1. The diffraction pattern of PA6 (Figure 1 curve a) is typical for polyamide. There are two monoclinic α-phases (α(002) at 2θ = 24.1° and α(200) at 2θ = 20.0°), as well as a hexagonal phase γ(200) at 2θ = 21.75°. Diffractograms of PA6/MMT-PVP nanocomposites (Figure 1 curve b–d) have a similar crystal structure. However, the reflex intensity of the γ-phase significantly decreases if the MMT-PVP content increase and slight shifts of the reflexes of α-phases are also observed. The γ-phase reflex almost disappears with an MMT-PVP content of 20 wt%. Such differences may indicate a physical interaction between the nanocomposite components in the formic acid solution [33]. Crystalline reflections of MMT in the diffractograms of the developed nanocomposites are completely absent. This is explained

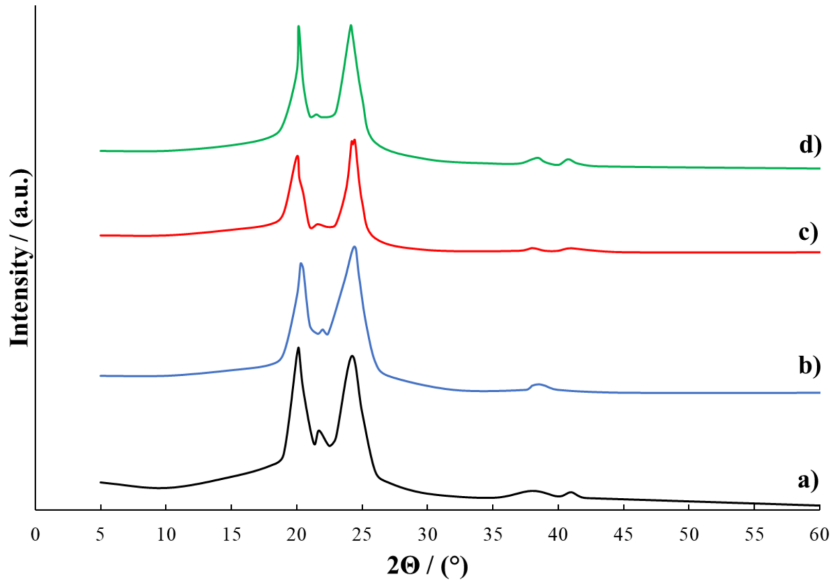

Fig. 1. X-ray diffraction patterns of PA6 and PA6/MMT-PVP nanocomposites obtained in solution: (a) PA6; (b) PA6 with 5 wt% MMT-PVP; (c) PA6 with 10 wt% MMT-PVP; (d) PA6 with 20 wt% MMT-PVP

by the complete exfoliation of nanoclay sheets in the polymer matrix and the transition of MMT to the amorphous phase. It is also obvious that small amounts of modified MMT almost do not affect the supramolecular structure of PA6 during the nanocomposite preparation in solution.

After additional thermomechanical processing of PA6/MMT-PVP nanocomposites on a capillary viscometer at 230±5 °C and a load of 5 kg, the appearance of their diffractograms changed significantly (Figure 2). Reflexes of monoclinic phases $\alpha(200)$ and $\alpha(002)$ have become significantly closer ($\alpha(200)$ phase shifted to $2\theta = 20.37–20.41°$, $\alpha(002)$ phase shifted to $2\theta = 23.46–23.75$). The biggest convergence of PA6 monoclinic phases is observed at the MMT-PVP content of 20 wt% (Figure 2 curve c). In addition, there was also a shift to the region of smaller 2θ angles of the γ-phase reflex (to $2\theta = 21.09–21.4°$, depending on the MMT-PVP content). After additional thermomechanical treatment of the samples, the reflex intensity of the γ-phases is lower than before treatment. It is worth noting that on the diffractogram of the nanocomposite PA6/MMT-PVP = 80/20, w/w after thermomechanical treatment, a clearly expressed crystalline reflex appeared at $2\theta = 29.31°$ (Figure 2 curve c), which is characteristic of MMT [30]. Such a crystalline reflex is absent in the diffractograms of the other studied nanocomposites. Therefore, it can be stated that during the thermomechanical processing of the samples, a more intensive physical interaction occurs between the nanocomposite components. Namely, interpolymer complexes are formed with physical bonds between PA6, exfoliated MMT sheets, and PVP macromolecules. As a result, the crystal structure of the formed nanocomposites also changes. Such conclusions are also supported by the DSC-TGA results presented below.

Thermograms and mass loss curves of nanocomposite samples and original PA6 are presented in Figure 3a-d, and thermomechanically treated nanocomposite samples in Figure 4a-c. The thermal characteristics of the samples are presented in Table 1. The first endopeak on the thermograms of the samples in the temperature range of 45–80 °C occurs consequently of the physical transition of polyamide from the glassy to the highly elastic state. The glass transition temperature (T_g) of the initial PA6 obtained in a formic acid solution is ~49 °C (Figure 3a, Table 1). Such data correlate well with known literature data, indicating the glass transition temperature of unfilled PA6 in the 46–53 °C [34–36]. Nanocomposites with 5 and 10 wt% MMT-PVP show an increase of 7 °C in the glass transition temperature compared to the original PA6. The sample PA6/MMT-PVP = 80/20, w/w, has a glass transition temperature close to the original PA6 (~47 °C). However, after thermomechanical treatment, the T_g of this sample increases significantly (to ~69 °C) and is almost similar to the T_g of nanocomposites with MMT-PVP content of 5 and 10 wt%. In general, the glass transition temperature of PA6 in

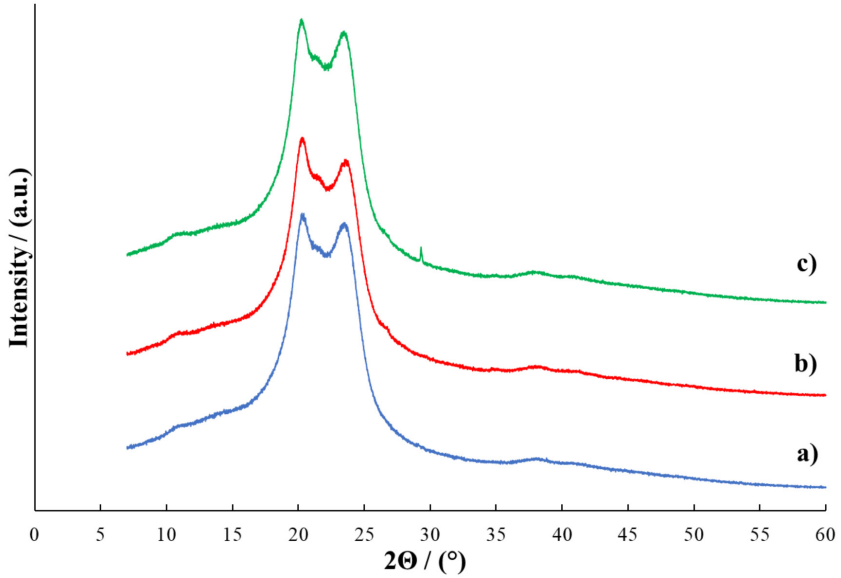

Fig. 2. X-ray diffraction patterns for PA6/MMT-PVP nanocomposites obtained in solution after additional thermomechanical treatment: (a) PA6 with 5 wt% MMT-PVP; (b) PA6 with 10 wt% MMT-PVP; (c) PA6 with 20 wt% MMT-PVP

Table 1. Results of DSC-TGA analysis for nanocomposites PA6/MMT-PVP

Sample	T_g, °C	T_m, °C	ΔH_m, J/g	X_c, %	Δg, %
PA6	49	214	86.4	37.6	2.3
PA6/MMT-PVP = 95/5, w/w	56	222	117.4	51.0	0.9
PA6/MMT-PVP = 90/10, w/w	56	224	139.1	60.5	2.4
PA6/MMT-PVP = 80/20, w/w	47	220	100.5	43.7	3.9
PA6/MMT-PVP = 95/5, w/w, thermomechanically treated	68	225	83.6	36.3	2.5
PA6/MMT-PVP = 90/10, w/w, thermomechanically treated	71	227	71.1	30.9	3.2
PA6/MMT-PVP = 80/20, w/w, thermomechanically treated	69	224	83.0	36.1	3.3

Note: T_g – glass transition temperature, °C; T_m – melting temperature, °C; ΔH_m – melting enthalpy, J/g; X_c – crystallinity degree, %; Δg – sample mass loss when heated from 40 to 275 °C, %.

nanocomposites that underwent thermomechanical treatment is significantly higher than in nanocomposites without thermomechanical treatment (by 12-15 °C) and the original PA6 (by 20 °C). This indicates the difficulty of getting PA6-based nanocomposites with a homogeneous distribution of modified MMT when mixing in a formic acid solution. Such nanocomposites require additional thermomechanical processing, especially mixing in a melt, before being processed into products.

DSC analysis of the original PA6 sample shows a single melting peak at 214 °C (Figure 3a, Table 1). The typical melting temperatures of γ and α structures of PA6 are ~212 and 222 °C, respectively [1]. The samples of all investigated PA6/MMT-PVP nanocomposites also show a single melting peak at temperatures higher than 220 °C (Table 1, Figure 3b-d, Figure 4a-c), which corresponds to the melting of α structures of PA6. Therefore, it can be stated that MMT-PVP during the modification of PA6 in formic acid solution contributes to PA6 crystal structures transformation from γ-form to thermodynamically more stable α-forms. The highest melting temperature of 224 °C is PA6 with MMT-PVP content of 10 wt%. The melting point of all investigated PA6/MMT-PVP nanocomposites slightly increases after thermomechanical treatment (Table 1).

According to the recorded melting enthalpy of the samples (Table 1, Figures 3, 4), the crystallinity degree of PA6 in nanocomposites was determined. The crystallinity degree of the original PA6 is ~38%. The crystallinity degree of PA6 in nanocomposites is significantly affected by the MMT-PVP content and additional thermomechanical processing. The addition of MMT-PVP to PA6 increases its crystallinity degree. Moreover, the highest crystallinity degree (~61%) has PA6 with an MMT-PVP content of 10 wt%. When the MMT-PVP content in PA6 is increased to 20 wt% the

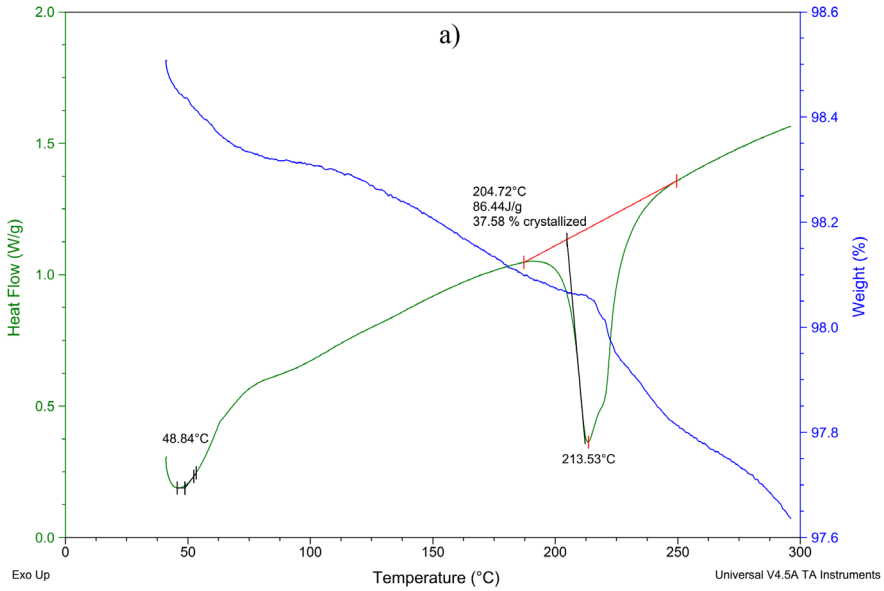

Fig. 3. DSC-TG curves of PA6 (a)

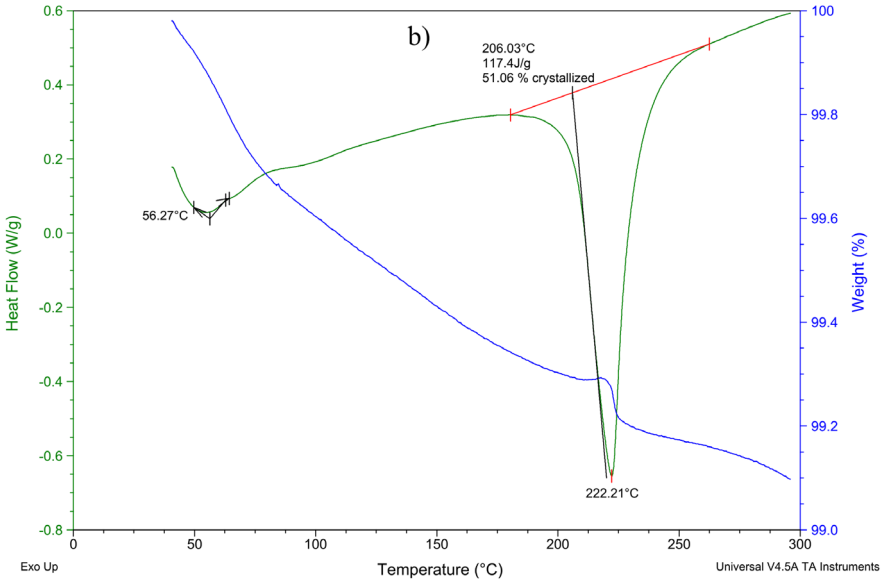

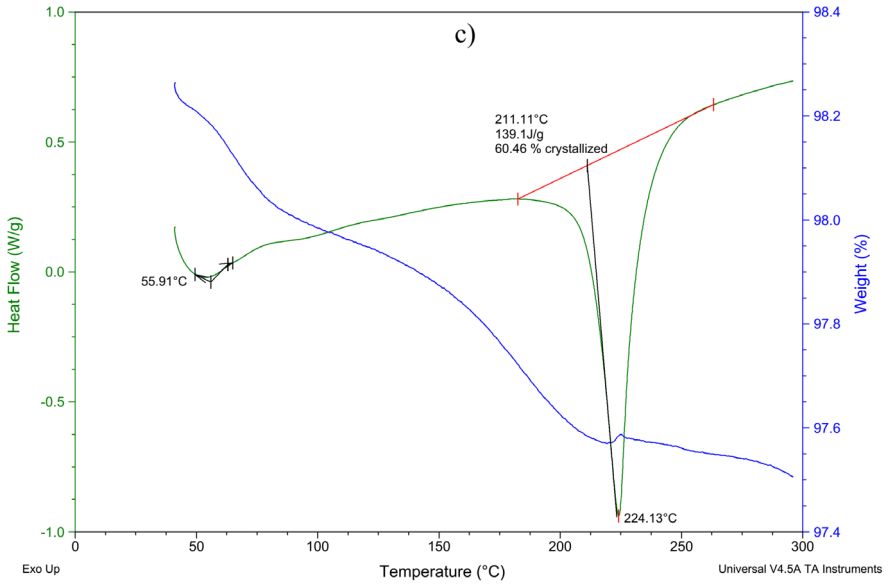

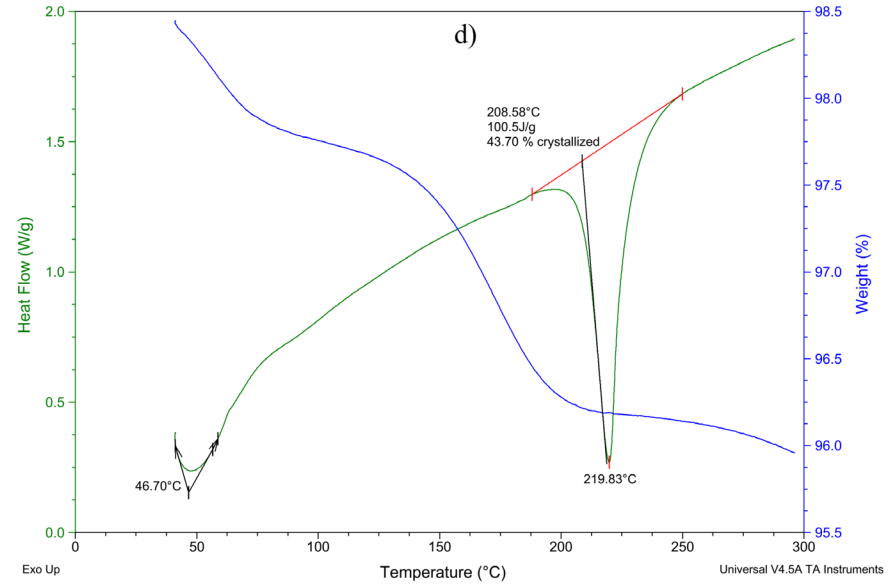

Fig. 3. Cont. DSC-TG curves of PA6 with 5 wt% MMT-PVP (b), PA6 with 10 wt% MMT-PVP (c), PA6 with 20 wt% MMT-PVP (d)

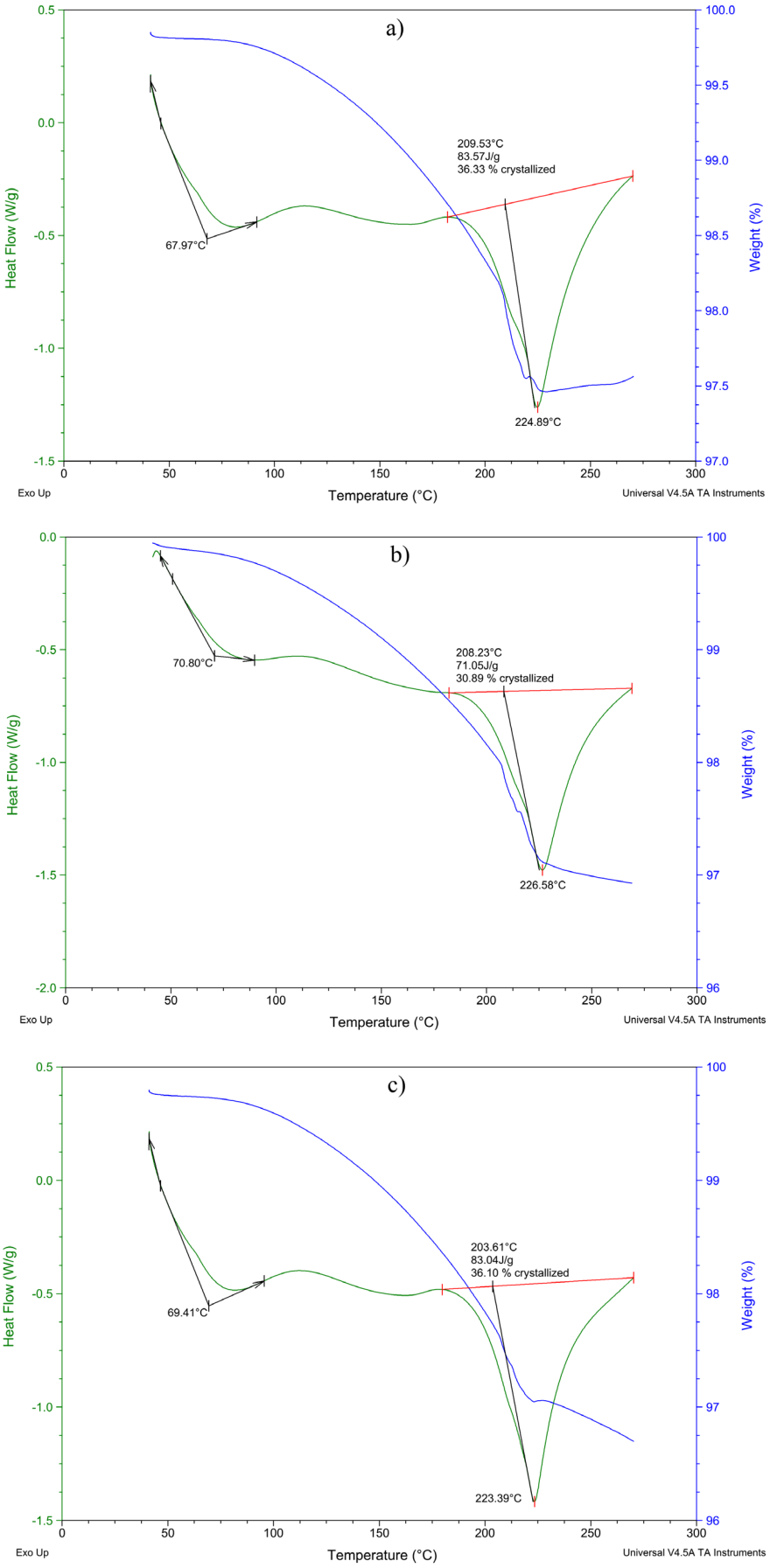

Fig. 4. DSC-TG curves of the samples after thermomechanical treatment: (a) PA6 with 5 wt% MMT-PVP; (b) PA6 with 10 wt% MMT-PVP, w/w; (c) PA6 with 20 wt% MMT-PVP

crystallinity degree decreases to ~44%, and with an MMT-PVP content of 5 wt% the crystallinity degree is ~51%. That is, it can be stated that the optimal content of modified MMT in PA6 for the nucleation and growth of α crystals is 10 wt%. After thermomechanical processing of PA6/MMT-PVP nanocomposites at 230 °C, their crystallinity degree significantly decreased (Figure 4, Table 1) and is lower than the original PA6 crystallinity degree. In addition, a broad endopeak appeared in the temperature range of 110–170 °C on the thermograms of thermomechanically treated nanocomposites (Figure 4). This can be explained by the fact that during thermomechanical treatment, in the process of melting the nanocomposite, the destruction of the crystal structure and depolymerization of PA6 occur with the formation of caprolactam and oligomers, which melt in the temperature range of 110-170 °C. Consequently of these processes, the crystallinity degree of PA6 in thermomechanically treated nanocomposites decreases.

The mass loss of the original PA6 sample during heating from 40 to 275 °C is 2.3% and is mainly associated with the evaporation of physically bound water and the remains of solvents used in the sample preparation. The mass loss of nanocomposite samples in this temperature range increases from 0.9% to 3.9% with an increase in the content of MMT-PVP in nanocomposites from 5 to 20 wt%, respectively (Table 1, Figures 3, 4). This is due to the increasing PVP content and its partial oxidation-reduction destruction during heating. PA6 with MMT-PVP content of 5 wt% has the lowest mass loss (0.9%), but after thermomechanical treatment, the mass loss of such a sample increased to 2.5%. After thermomechanical treatment, the mass loss of PA6 with MMT-PVP content of 10 wt% also increases. The increase in mass loss of nanocomposite samples after thermomechanical treatment can be explained by the partial destruction of PA6 and PVP during such treatment.

The above-described changes in the structure of PA6 due to modification with MMT-PVP significantly affect the technological properties of nanocomposites (Table 2). The Vicat softening temperature (T_V) of PA6/MMT-PVP nanocomposites varies similarly to the melting temperature change. That is, after additional thermomechanical processing of nanocomposites, it increases significantly. The thermomechanically treated PA6 with MMT-PVP content of 10 wt% has the highest softening temperature, its T_V is 36 °C higher than PA6. It can be assumed that as a result of additional heat treatment, a more ordered and dense nanocomposite structure is formed, which softens at higher temperatures.

The MFI of PA6/MMT-PVP nanocomposites is significantly higher than the MFI of PA6 and increases with increasing MMT-PVP content. However, after additional thermomechanical treatment, the MFI of these nanocomposites decreases. Such changes in the fluidity of nanocomposites correlate well with changes in the PA6 crystal structure and melting temperature. Therefore, PA6/MMT-PVP nanocomposites obtained from a solution have high fluidity, which indicates their manufacturability. This will make it possible to manufacture structural products of various configurations by injection molding.

CONCLUSIONS

The structure, crystallization behavior, and thermal properties of PA6/MMT-PVP nanocomposites obtained from the solution were investigated in the work, and the effect of additional thermomechanical processing of nanocomposites on these characteristics was determined. Using the XRD and DSC methods, it was established that during the preparation of PA6/MMT nanocomposites in a formic acid solution, thermodynamically stable α-phases of PA6 are the dominant crystal structures. The reflex

Table 2. Technological properties of nanocomposites PA6/MMT-PVP

Sample	$MFI_{230°C/2.16\ kg}$, g/10 min	T_V,, °C
PA6	24±0.5	155±1
PA6/MMT-PVP = 95/5, w/w	29±0.5	160±1
PA6/MMT-PVP = 90/10, w/w	36±0.5	165±1
PA6/MMT-PVP = 80/20, w/w	66±0.9	165±1
PA6/MMT-PVP = 95/5, w/w, thermomechanically treated	21±0.5	173±1
PA6/MMT-PVP = 90/10, w/w, thermomechanically treated	23±0.5	191±1
PA6/MMT-PVP = 80/20, w/w, thermomechanically treated	49±0.8	187±1

intensity of the hexagonal phase γ decreases with increasing MMT-PVP content in nanocomposites, and after thermomechanical treatment at 230 °C, these reflexes almost disappear. The crystallinity degree of PA6 in the nanocomposites is significantly higher than the crystallinity degree of the original PA6. Modified MMT in nanocomposites is in an amorphous phase, which indicates its complete exfoliation. Additional thermomechanical treatment of PA6/MMT nanocomposites significantly affects their structure and thermal properties. In particular, the nanocomposite glass transition, softening and melting temperatures increase, but the crystallinity degree decreases due to the partial depolymerization of PA6. The obtained results and described crystallization phenomena of PA6 in nanocomposites based on modified MMT make it possible to understand and predict the mechanical behavior of products made of such nanocomposites, including at elevated temperatures. In addition, the obtained nanocomposites have high manufacturability. It is known that PA6 is a material from which structural products are mainly made by injection molding. Wide use of polyamide materials in the manufacture of mechanically responsible parts of machines, particularly in the automotive industry, requires the ability of the material to maintain the product shape at elevated temperatures. Therefore, the experimental results obtained in the work have important practical significance.

Acknowledgment

The work was carried out within the framework of the National Scholarship Program of the Slovak Republic.

REFERENCES

1. Yebra-Rodríguez A., Alvarez-Lloret P., Rodríguez-Navarro A. B., Martín-Ramos J. D., Cardell C. Thermo-XRD and differential scanning calorimetry to trace epitaxial crystallization in PA6/montmorillonite nanocomposites. Materials Letters 2009; 63(13-14): 1159-1161. https://doi.org/10.1016/j.matlet.2009.02.027
2. Krasinskyi V., Suberlyak O., Sikora J., Zemke V. Nanocomposites based on polyamide-6 and montmorillonite intercalated with polyvinylpyrrolidone. Polymer-Plastics Technology and Materials 2021; 60(15): 1641–1655. https://doi.org/10.1080/25740881.2021.1924201
3. Goettler L. A., Lee K. Y., Thakkar H. Layered silicate reinforced polymer nanocomposites: Development and applications. Polymer Reviews 2007; 47(2): 291–317. https://doi.org/10.1080/15583720701271328
4. Dulebová Ľ., Greškovič F., Sikora J. W., Krasinskyi V. Analysis of the mechanical properties change of PA6/MMT nanocomposite system after ageing. Key Engineering Materials 2017; 756: 52–59. https://doi.org/10.4028/www.scientific.net/KEM.756.52
5. Lai D., Li Y., Wang C., Liu Y., Li D., Yang J. Inhibition effect of aminated montmorillonite on crystallization of dendritic polyamide 6. Materials Today Communications 2020; 25: 101578. https://doi.org/10.1016/j.mtcomm.2020.101578
6. Siddique S., Leung P. S., Njuguna J. Drilling oil-based mud waste as a resource for raw materials: A case study on clays reclamation and their application as fillers in polyamide 6 composites. Upstream Oil and Gas Technology 2021; 7: 100036. https://doi.org/10.1016/j.upstre.2021.100036
7. Cheira M. F., Kouraim M. N., Zidan I. H., Mohamed W. S., Hassanein T. F. Adsorption of U(VI) from sulfate solution using montmorillonite/polyamide and nano-titanium oxide/polyamide nanocomposites. Journal of Environmental Chemical Engineering 2020; 8(5): 104427. https://doi.org/10.1016/j.jece.2020.104427
8. Usuki A., Kojima Y., Kawasumi M., Okada A., Fukushima Y., Kurauchi T., Kamigaito O. Synthesis of nylon 6-clay hybrid. Journal of Materials Research 1993; 8: 1179–1184. https://doi.org/10.1557/JMR.1993.1179
9. Chen H.-B., Schiraldi, D. A. Flammability of polymer/clay aerogel composites: An overview. Polymer Reviews 2018; 59(1): 1–24. https://doi.org/10.1080/15583724.2018.1450756
10. Jeon H. G., Jung H.-T., Lee S. W., Hudson S. D. Morphology of polymer/silicate nanocomposites. Polymer Bulletin 1998; 41: 107–113. https://doi.org/10.1007/s002890050339
11. Giannelis E. P. Polymer layered silicate nanocomposites. Advanced Materials 1996; 8(1): 29–35. https://doi.org/10.1002/adma.19960080104
12. El Achaby M., Ennajih H., Arrakhiz F. Z., El Kadib A., Bouhfid R., Essassi E., Qaiss A. Modification of montmorillonite by novel geminal benzimidazolium surfactant and its use for the preparation of Polymer Organoclay nanocomposites. Composites Part B: Engineering 2013; 51: 310–317. https://doi.org/10.1016/j.compositesb.2013.03.009
13. García-López D., Gobernado-Mitre I., Fernández J. F., Merino J. C., Pastor J. M. Influence of clay modification process in PA6-layered silicate nanocomposite properties. Polymer 2005; 46(8): 2758–2765. https://doi.org/10.1016/j.polymer.2005.01.038
14. Hwang S., Liu S., Hsu P. P., Yeh J., Yang J., Chang K., Chu, S. Effect of organoclay and preparation methods on the mechanical/thermal properties of microcellular injection molded polyamide 6-clay nanocomposites. International Communications in Heat

and Mass Transfer 2011; 38(9): 1219–1225. https://doi.org/10.1016/j.icheatmasstransfer.2011.06.013

15. Yebra-Rodriguez A., Alvarezl-Lloret P., Cardell C., Rodriguez-Navarro A. Crystalline properties of injection molded polyamide-6 and polyamide-6/montmorillonite nanocomposites. Applied Clay Science 2009; 43(1): 91–97. https://doi.org/10.1016/j.clay.2008.07.010
16. Krasinskyi V., Gajdos I., Suberlyak O., Antoniuk V., Jachowicz T. Study of the structure and thermal characteristics of nanocomposites based on polyvinyl alcohol and Intercalated Montmorillonite. Journal of Thermoplastic Composite Materials 2021; 34(12): 1680–1691. https://doi.org/10.1177/0892705719879199
17. Oulidi O., Nakkabi A., Elaraaj I., Fahim M., Moualij N. E. Incorporation of olive pomace as a natural filler in to the PA6 matrix: Effect on the structure and thermal properties of synthetic polyamide 6. Chemical Engineering Journal Advances 2022; 12: 100399. https://doi.org/10.1016/j.ceja.2022.100399
18. Guo H., Wang J., Zhou C., Zhang W., Wang Z., Xu B., Li J., Shang Y., de Claville Christiansen J., Yu D., Wu Z., Jiang S. Direct investigations of deformation and yield induced structure transitions in polyamide 6 below glass transition temperature with WAXS and saxs. Polymer 2015; 70: 109–117. https://doi.org/10.1016/j.polymer.2015.06.013
19. Follain N., Alexandre B., Chappey C., Colasse L., Médéric P., Marais S. Barrier properties of Polyamide 12/montmorillonite nanocomposites: Effect of clay structure and mixing conditions. Composites Science and Technology 2016; 136: 18–28. https://doi.org/10.1016/j.compscitech.2016.09.023
20. Xenopoulos A, Clark E. S. Physical structures. Nylon Plastics Handbook. Hanser Publishers, Munich, 1995.
21. Sun H., Jiang F., Lei F., Chen L., Zhang H., Leng J., Sun D. Graphite fluoride reinforced PA6 composites: Crystallization and mechanical properties. Materials Today Communications 2018; 16: 217–225. https://doi.org/10.1016/j.mtcomm.2018.06.007
22. Wei P., Cui S., Bai S. In situ exfoliation of graphite in solid phase for fabrication of graphene/polyamide-6 composites. Composites Science and Technology 2017; 153: 151–159. https://doi.org/10.1016/j.compscitech.2017.10.009
23. Xu S., Zhou J., Pan P. Strain-induced multiscale structural evolutions of crystallized polymers: From fundamental studies to recent progresses. Progress in Polymer Science 2023; 140: 101676. https://doi.org/10.1016/j.progpolymsci.2023.101676
24. Uematsu H., Kawasaki T., Koizumi K., Yamaguchi A., Sugihara S., Yamane M., Kawabe K., Ozaki Y., Tanoue S. Relationship between crystalline structure of polyamide 6 within carbon fibers and their mechanical properties studied using micro-raman spectroscopy. Polymer 2021; 223: 123711. https://doi.org/10.1016/j.polymer.2021.123711
25. Kumar Jain P. A., Sattar S., Mulqueen D., Pedrazzoli D., Kravchenko S. G., Kravchenko O. G. Role of annealing and isostatic compaction on mechanical properties of 3D printed short glass fiber nylon composites. Additive Manufacturing 2022; 51: 102599. https://doi.org/10.1016/j.addma.2022.102599
26. Miri V., Persyn O., Seguela R., Lefebvre J. M. On the deformation induced order–disorder transitions in the crystalline phase of polyamide 6. European Polymer Journal 2011; 47(1): 88–97. https://doi.org/10.1016/j.eurpolymj.2010.09.006
27. Sun L., Yang J.-T., Lin G.-Y., Zhong M.-Q. Crystallization and thermal properties of polyamide 6 composites filled with different nanofillers. Materials Letters 2007; 61(18): 3963–3966. https://doi.org/10.1016/j.matlet.2006.12.090
28. Lin J.-H., Pan Y.-J., Hsieh C.-T., Huang C.-H., Lin Z.-I., Chen Y.-S., Su K.-H., Lou C.-W. Using multiple melt blending to improve the dispersion of montmorillonite in polyamide 6 nanocomposites. Polymer Testing 2016; 56: 74–82. https://doi.org/10.1016/j.polymertesting.2016.09.016
29. Monticelli O., Musina Z., Frache A., Bellucci F., Camino G., Russo S. Influence of compatibilizer degradation on formation and properties of PA6/Organoclay Nanocomposites. Polymer Degradation and Stability 2007; 92(3): 370–378. https://doi.org/10.1016/j.polymdegradstab.2006.12.010
30. Krasinskyi V., Suberlyak O., Dulebová Ľ., Antoniuk V. Nanocomposites on the basis of thermoplastics and montmorillonite modified by polyvinylpyrrolidone. Key Engineering Materials 2017; 756: 3–10. https://doi.org/10.4028/www.scientific.net/KEM.756.3
31. Wunderlich B. Macromolecular physics, vol. 3, chap. 8: crystal melting. Academic Press, New-York, 1971.
32. Millot C., Fillot L.-A., Lame O., Sotta P., Seguela R. Assessment of polyamide-6 crystallinity by DSC. Journal of Thermal Analysis and Calorimetry 2015; 122: 307–314. https://doi.org/10.1007/s10973-015-4670-5
33. Levytskyj V., Kochubei V., Gancho A. Influence of the silicate modifier nature on the structure and properties of polycaproamide. Chemistry & Chemical Technology 2013; 7(2): 169–173. https://doi.org/10.23939/chcht07.02.169
34. Ksouri I., Haddar N. Long term ageing of Polyamide 6 and polyamide 6 reinforced with 30% of glass fibers: Temperature effect. Journal of Polymer Research 2018; 25: 153. https://doi.org/10.1007/s10965-018-1551-1
35. Forster M. J. Glass transition temperature of Nylon 6. Textile Research Journal 1968; 38(5): 474–480. https://doi.org/10.1177/004051756803800504
36. Krasinskyi V., Kochubei V., Klym Y., Suberlyak O. Thermogravimetric research into composites based on the mixtures of polypropylene and modified polyamide. Eastern-European Journal of Enterprise Technologies 2017; 4(12(88): 44–50. https://doi.org/10.15587/1729-4061.2017.108465